Oesterhelt, D., & Krippahl, G. (1973) *FEBS Lett. 36*, 72–76.
Oesterhelt, D., & Stoeckenius, W. (1973) *Proc. Natl. Acad. Sci. U.S.A. 70*, 2853–2857.
Oesterhelt, D., & Stoeckenius, W. (1974) *Methods Enzymol. 31*, 667–678.
Ort, D. R., & Parson, W. W. (1978) *J. Biol. Chem. 253*, 6158–6164.
Ort, D. R., & Parson, W. W. (1979) *Biophys. J. 25*, 341–354.
Ovchinnikov, Y. A., Abdulaev, N. G., Feigina, M. Y., Kiselev, A. V., & Lobanov, N. A. (1979) *FEBS Lett. 100*, 219–224.
Rafferty, Ch. N. (1979) *Photochem. Photobiol. 29*, 109–120.
Rott, R., & Avi-Dor, Y. (1977) *FEBS Lett. 81*, 267–270.
Schreckenbach, Th., Fischer, U., Knobling, A., & Oesterhelt, D. (1977) *FEBS Meeting, Copenhagen, 11th*, Abstr. A4-13 L1 9.
Schulten, K., & Tavan, P. (1977) *Nature (London) 722*, 85–86.
Slifkin, M. A., Garty, H., Sherman, W. V., Vincent, M. F. P., & Caplan, S. R. (1979) *Biophys. Struct. Mech. 5*, 313–320.
Stockburger, M., Klusmann, W., Gattermann, H., Massig, G., & Peters, R. (1979) *Biochemistry 18*, 4886–4900.
Stoeckenius, W. (1978) in *Energetics and Structure of Halophilic Microorganisms* (Caplan, S. R., & Ginsburg, M., Eds.) pp 185–198, Elsevier-North-Holland Biomedical Press, Amsterdam.
Stoeckenius, W., Lozier, R. H., & Bogomolni, R. A. (1979) *Biochim. Biophys. Acta 505*, 215–278.
Trissl, H.-W., & Montal, M. (1977) *Nature (London) 266*, 655–657.
Unwinn, P. N. T., & Henderson, R. (1975) *J. Mol. Biol. 94*, 425–440.
Wagner, G., & Hope, A. B. (1976) *Aust. J. Plant Physiol. 3*, 665–676.

X-ray Diffraction and Calorimetric Study of Anhydrous and Hydrated *N*-Palmitoylgalactosylsphingosine (Cerebroside)†

M. J. Ruocco, D. Atkinson, D. M. Small, R. P. Skarjune, E. Oldfield, and G. G. Shipley*

ABSTRACT: Differential scanning calorimetry and X-ray diffraction of anhydrous and hydrated *N*-palmitoylgalactosylsphingosine (NPGS) show evidence of complex polymorphic behavior and interconversions between stable and metastable structural forms. Anhydrous NPGS exhibits three lamellar crystal forms (A, B, and B′) at temperatures below 143 °C and a liquid-crystal form between 143 and 180 °C before melting to an isotropic liquid at 180 °C. The crystal B → liquid-crystal transition is accompanied by an enthalpy change, ΔH, of 11.2 kcal/mol of NPGS, while a relatively small enthalpy change (ΔH = 0.8 kcal/mol) marks the liquid-crystal → liquid transition. The A and B′ crystal forms do not hydrate readily at room temperature. When heated, crystal form A in the presence of water undergoes an exothermic transition at 52 °C to produce a thermodynamically stable hydrated crystal E form. X-ray diffraction shows that this stable bilayer crystal form has a highly ordered hydrocarbon chain packing arrangement; melting to the bilayer liquid-crystal form occurs at 82 °C with a large enthalpy change, ΔH = 17.5 kcal/mol of NPGS. A complex liquid-crystal → crystal transition is observed on cooling; the cooling rate independent exotherm involves the transition of the hydrated liquid crystal to an intermediate metastable crystal form identical with anhydrous crystal form A. The subsequent cooling rate dependent step involves the conversion of the metastable crystal form A to the stable crystal form E. We suggest that hydrated crystal form E is stabilized by both a highly ordered chain packing mode and a lateral intermolecular hydrogen bonding network involving the sphingosine backbone, the galactosyl group, and interbilayer water molecules. Although disruption of both the specific hydrocarbon chain packing and H-bonding networks occurs at the high enthalpy transition to the bilayer liquid-crystal Lα form, these two types of interactions are not reestablished simultaneously on cooling. First, recrystallization of the hydrocarbon chains accompanies removal of water from the lipid interface, leading to "dehydrated" metastable crystal form A. This is followed by a time-dependent, temperature-dependent hydration process which allows a rearrangement of the hydrogen-bonding matrix. Alterations in the NPGS–NPGS and NPGS–water interactions accompany further changes in the hydrocarbon chain packing and lead to the formation of the stable E form.

Sphingolipids, including glycosphingolipids and sphingomyelin, are derived from the long-chain, aliphatic base sphingosine and differ structurally from the glycerol-based phospholipids and glycolipids. Glycosphingolipids are present in most animal cell membranes, albeit usually in relatively small amounts. Specific examples of this lipid class include globosides, which occur in tissues of the kidney, heart, and the reticuloendothelial system, and gangliosides, which occur in a number of tissues acting as receptors for hormones and toxins (Fishman & Brady, 1976). Some tissues, however, contain relatively large amounts of glycosphingolipids; for example, the myelin sheath of the central and peripheral nervous system has as its major (20% dry weight) polar lipid *N*-acyl-1-*O*-β-D-galactosylsphingosine or galactocerebroside (Johnson et al., 1948; Lapetina et al., 1968). The structural and/or functional role of this glycosphingolipid in the myelin membrane remains to be established.

Pronounced glycosphingolipid accumulation in various tissues (brain, liver, spleen, etc.) can result as a consequence of

† From the Biophysics Institute, Departments of Medicine and Biochemistry, Boston University School of Medicine, Boston, Massachusetts 02118 (M.J.R., D.A., D.M.S., and G.G.S.), and the School of Chemical Sciences, University of Illinois at Urbana—Champaign, Urbana, Illinois 61801 (R.S. and E.O.). *Received March 24, 1981.* This investigation was supported by Research Grants HL-18623, HL-07291, and HL-19481 from the National Institutes of Health and Research Grant PCM 76-01491 from the National Science Foundation. D.A. is an Established Investigator of the American Heart Association.

0006-2960/81/0420-5957$01.25/0

aberrant enzymatic pathways for catabolism of these lipids, leading to a variety of pathological disorders. Complex sphingolipidoses which result from accumulating glycosphingolipids include Fabry's disease (globoside), metachromatic leukodystrophy (cerebroside sulfate), gangliosidoses (GM_1 and GM_2 gangliosides), Gaucher's disease (glucosylceramide), and Krabbe's disease (galactosylceramide) [see, for example, Brady (1978)].

Although the structure and thermotropic behavior of membrane phospholipids have been studied extensively by X-ray/neutron diffraction, differential scanning calorimetry, and spectroscopic methods (NMR, ESR, fluorescence, etc.), few systematic studies of sphingolipids have been reported. Sphingomyelin has been shown to exhibit bilayer structures and thermotropic behavior similar to, but not identical with, phospholipids such as phosphatidylcholine (Shipley et al., 1974; Barenholz et al., 1976; Untracht & Shipley, 1977; Calhoun & Shipley, 1979; Neuringer et al., 1979). An unusual property of hydrated C_{18}-sphingomyelin is its formation of a metastable bilayer structure. This metastable form converts to a stable bilayer form with an unusually ordered structure due either to variation in degree of hydration or to increased hydrogen bonding between adjacent sphingomyelin molecules (Estep et al., 1980).

For glycosphingolipids, cerebrosides have received the most attention. Ox brain cerebrosides containing predominantly $C_{24:0}$, $C_{24:1}$, and $C_{18:0}$ fatty acids linked to the C_{18}-sphingosine base were shown by X-ray diffraction to undergo a hydrocarbon chain melting transition at relatively high temperatures, in the 65–70 °C range (Reiss-Husson, 1967). Similar conclusions concerning thermotropic behavior of cerebrosides were derived by Clowes et al. (1971), Oldfield & Chapman (1972), and Abrahamsson et al. (1972). The most systematic approach to understanding the structure of sphingolipids has been that of Abrahamsson, Pascher, and co-workers. They showed by X-ray diffraction that homogeneously acylated sphingolipids including cerebrosides formed a number of complex thermotropic and lyotropic mesophases (Abrahamsson et al., 1972). Furthermore, comparison of the crystal structures of ceramide (Dahlen & Pascher, 1972), psychosine (Abrahamsson et al., 1977), *N*-(2-hydroxyoctadecanoyl)galactosyldihydrosphingosine (Pascher & Sundell, 1977), and other sphingolipid constituents suggested that the hydrogen-bonding capacity of the sphingosine moiety could result in intermolecular interactions different from those exhibited by phospholipids and could be of functional importance in biomembranes (Pascher, 1976).

Other naturally occurring glycosphingolipids have been studied by X-ray diffraction, calorimetric and spectroscopic methods (Curatolo et al., 1977; McCabe & Green, 1977; Correa-Freire et al., 1979; Bunow, 1979), and complex phase behavior and thermotropic properties have been found. Recently a number of galactosyl- and glucosylceramides with specific *N*-acyl linked fatty acids have been synthesized (Skarjune & Oldfield, 1979). Specific deuterium labeling in both the fatty acyl region and the sugar head group has led to deuterium magnetic resonance studies of cerebroside conformation and dynamics (Skarjune & Oldfield, 1979; Huang et al., 1980). In this paper, we present findings from an X-ray diffraction and calorimetric study of the phase behavior of *N*-palmitoylgalactosylsphingosine (NPGS)[1] in both the anhydrous and hydrated state.

Materials and Methods

Samples. *N*-Palmitoylgalactosylsphingosine[2] was synthesized by starting from pig brain cerebroside according to methods described by Skarjune & Oldfield (1979). It is estimated that NPGS contains approximately 5% of the dihydrosphingosine derivative. The purity was checked by thin-layer chromatography. The NPGS gave a single spot in the solvent system chloroform/methanol/water (65:25:4) and was used without further purification.

Anhydrous and lipid–water samples were prepared for polarizing microscopy, differential scanning calorimetry, and X-ray diffraction, as described under each technique.

Polarizing Microscopy. Samples of anhydrous NPGS were placed between a glass microscope slide and a coverslip. For hydrated samples, NPGS and water were weighed into a constricted tube, flame sealed under nitrogen, heated to 90 °C (a temperature above the chain melting transition; see Results), and centrifuged through the constriction several times in order to mix the two components. In some cases, the mixing was done at room temperature. An aliquot was placed on a microscope slide, covered with a coverslip, and sealed at the edges with epoxy resin. Samples were examined by direct and polarizing light with a Zeiss NL microscope fitted with a heating/cooling stage. Changes in optical texture and sample viscosity were determined during heating and cooling in the temperature range 0–190 °C.

Differential Scanning Calorimetry. Anhydrous samples were prepared by weighing NPGS into a stainless steel pan and hermetically sealing the pan. Hydrated samples were prepared similarly with subsequent introduction of double-distilled water by a microsyringe to make a 70 wt % water dispersion before the DSC pan was sealed. Heating and cooling scans over the temperature range −20 → 210 °C were performed on a Perkin-Elmer (Norwalk, CT) DSC-2 calorimeter calibrated with indium and gallium. Heating rates ranged from 0.31 to 40 °C/min. Isothermal modes were also utilized. Transition temperatures were determined as the onset of the transition extrapolated to the base line. Enthalpy measurements were determined from the area under the transition peak by comparison with those for a known standard (gallium). Base lines in the region of the transition were approximated by extrapolating the pretransition base line to the posttransition base line.

X-ray Diffraction. Anhydrous NPGS samples were placed in 1-mm (inner diameter) capillaries (Charles Supper Co., Natick, MA). Samples containing water were mixed in the constricted tube, centrifuged through the constriction at room temperature, and placed in the capillary tube. The capillary tubes were flame sealed and placed in a sample holder kept at constant temperature by a circulating solvent/water bath. Nickel-filtered Cu Kα X radiation (λ = 1.5418 Å) from an Elliot GX-6 rotating anode X-ray generator (Elliot Automation, Borehamwood, England) was focused by a toroidal mirror optical camera (Elliot, 1965). Diffraction patterns were recorded on Kodak No-Screen X-ray film. Microdensitometry of X-ray photographs was carried out on a Joyce-Loebl Model III-CS microdensitometer.

Results

(*A*) *Anhydrous N-Palmitoylgalactosylsphingosine. Polarizing Microscopy.* NPGS, crystallized from a chloroform–

[1] Abbreviations used: NPGS, *N*-palmitoylgalactosylsphingosine; DSC, differential scanning calorimetry.

[2] *N*-Palmitoylgalactosylsphingosine (NPGS) is used as a trivial name for *N*-hexadecanoyl-1-*O*-β-D-galactosylsphingosine or *N*-hexadecanoyl-1-*O*-β-D-galactosyl-4-sphingenine. This compound has also been referred to as *N*-palmitoylgalactosylceramide.

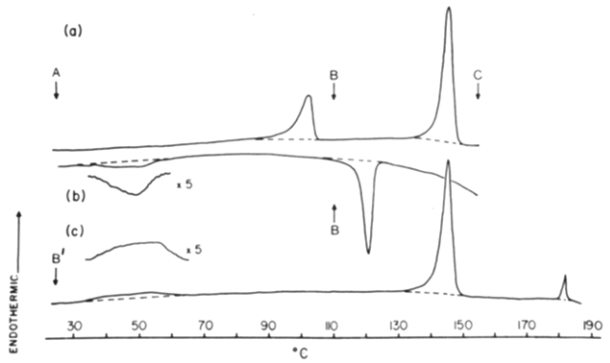

FIGURE 1: Differential scanning calorimetry of anhydrous NPGS. (a) Initial heating scan, 5 °C/min; (b) cooling scan, 5 °C/min [low-temperature exotherm is also shown at 5 × sensitivity of (b)]; (c) subsequent heating scan, 5 °C/min [low-temperature endotherm is also shown at 5 × sensitivity of (c)]. Lettered arrows indicate temperatures at which X-ray diffraction experiments were performed (see Figure 2).

methanol (10:1 v/v) solvent, is a white polycrystalline powder. Under the polarizing microscope at ambient temperatures, the sample exhibits a birefringent texture indicative of a crystalline structure. The birefringence persists throughout the heating range 23–143 °C, at which temperature (143 °C) conversion to a middle-textured liquid crystal occurs (Rosevear, 1954). The lipid is very maleable and softens as heating continues beyond 143 °C. At 180 °C, a second textural and viscosity change is observed with the formation of a fluid isotropic liquid.

Differential Scanning Calorimetry. The calorimetric behavior of the anhydrous cerebroside is summarized in Figure 1. The initial heating scan over the 20–160 °C range demonstrates two endothermic transitions (Figure 1a). The lower temperature endotherm occurs at 96 °C with an enthalpy ΔH of 6.2 ± 0.6 kcal/mol. The second transition at 143 °C has an enthalpy ΔH of 11.2 ± 0.3 kcal/mol. The immediate cooling scan (Figure 1b) from 160 °C exhibits a supercooled exothermic transition at 123 °C with an enthalpy of 9.7 ± 0.6 kcal/mol. The latter is significantly less than the transition enthalpy obtained at 143 °C on heating. When the cerebroside is further cooled, a broad low enthalpy exotherm centered at 48 °C (ΔH = 2.2 ± 0.1 kcal/mol) is observed. Subsequent heating (Figure 1c) shows this broad transition to be reversible, with the peak temperature slightly elevated (52 °C). No transition is observed at 96 °C, but the major endotherm at 143 °C remains. When the cerebroside is heated further, the liquid-crystal → isotropic liquid transition occurs at 180 °C, with an enthalpy of 0.8 ± 0.1 kcal/mol (Figure 1c). The calorimetric behavior shown in Figure 1b,c is the reproducible behavior of the anhydrous lipid once the initial 96 °C transition is exceeded and provided the liquid-crystal isotropic melt is not exceeded. The enthalpies of the transitions are slightly reduced on subsequent heating/cooling cycles due to the fact that some degradation of NPGS occurs at temperatures above 150 °C, as revealed by thin-layer chromatography [see also Abrahamsson et al. (1972)].

X-ray Diffraction. X-ray diffraction experiments to determine the structural changes at each transition were performed at temperature points below and above the calorimetric transitions. The X-ray patterns obtained at temperatures indicated by the lettered arrows (A–C) in Figure 1 are shown in Figure 2.

The X-ray diffraction pattern of NPGS at 23 °C demonstrates 12 orders of reflections indexing on a lamellar geometry, the even order reflections being much stronger than the odd

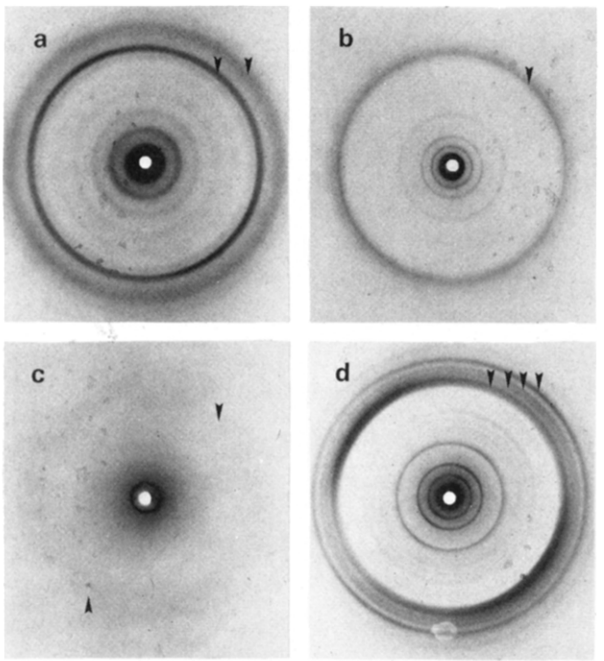

FIGURE 2: X-ray diffraction patterns of anhydrous NPGS at different temperatures. (a) T = 23 °C (prior to heating sample), crystal form A; (b) T = 110 °C, crystal form B; (c) T = 155 °C, liquid-crystalline phase; (d) T = 23 °C (after the sample was heated to 160 °C), crystal form B′.

orders (Figure 2a). The lamellar repeat distance, d, is 58.0 ± 0.5 Å. The wide angle reflections are characterized by a strong, sharp reflection at 1/4.4 Å^{-1} and a broader reflection centered at 1/3.8 Å^{-1} (see arrows in Figure 2a). When the lipid is heated beyond the 96 °C transition to 110 °C, the diffraction pattern changes (Figure 2b). A lamellar structure is still present, but the repeat distance decreases to 47.0 ± 0.5 Å. In the wide angle region, a sharp line centered at 1/4.4 Å^{-1} overlaps a more diffuse line (Figure 2b).

Above the large enthalpy transition, at 155 °C, the diffraction pattern exhibits a single sharp reflection at 1/33.5 Å^{-1} and a diffuse reflection at 1/4.6 Å^{-1} (Figure 2c). Cooling from the liquid-crystal phase through the transition at 123 °C to 110 °C gives the identical pattern with that obtained after heating (see Figure 2b). Further cooling to 23 °C gives the diffraction pattern shown in Figure 2d. Although the lamellar spacing remains unchanged at 47.0 ± 0.5 Å, the wide angle region shows a number of sharp reflections at 1/4.5, 1/4.17, 1/4.0, and 1/3.8 Å^{-1}, indicative of an altered hydrocarbon chain packing mode. This diffraction pattern, following the heating/cooling cycle, is clearly different from that originally observed at 23 °C. Heating to 110 °C (i.e., above the broad transition endotherm at 52 °C) produced a diffraction pattern identical with that shown in Figure 2b.

(*B*) *Hydrated N-Palmitoylgalactosylsphingosine. Polarizing Microscopy*. Addition of water to the anhydrous NPGS produces no lyotropic mesomorphism at ambient temperatures. Under the polarizing microscope, two phases, NPGS crystal form A and water, are observed. Heating the lipid in the presence of excess water showed no gross textural alterations until 82 °C, whereupon myelin figures, indicative of a lamellar liquid-crystalline phase, were observed.

Differential Scanning Calorimetry. The calorimetric behavior of cerebroside in the presence of excess (70 wt %) water is depicted in Figure 3. Figure 3a illustrates the behavior of NPGS placed in a DSC sample pan with water added, sealed, and examined immediately in the calorimeter. The heating and cooling rate is 5 °C/min. Two calorimetric transitions

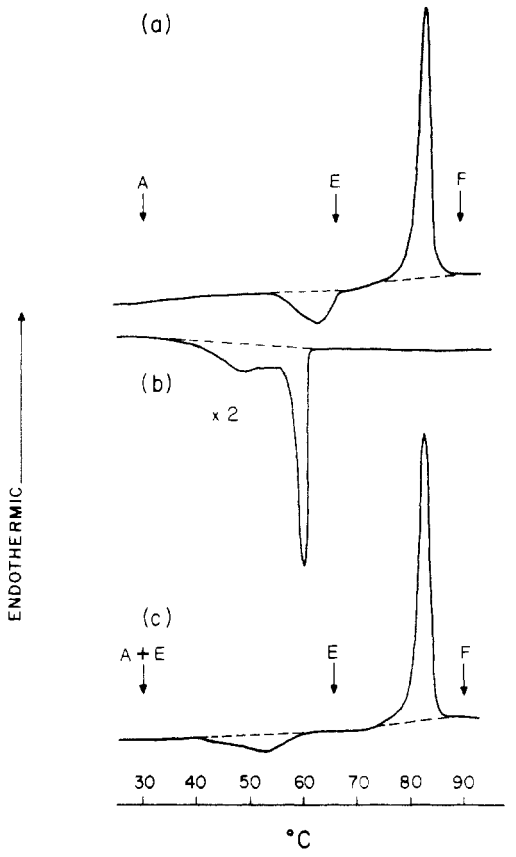

FIGURE 3: Differential scanning calorimetry of NPGS plus excess water (70 wt % water). (a) Initial heating scan, 5 °C/min; (b) cooling scan, 5 °C/min (×2 sensitivity); (c) subsequent heating scan immediately after cooling, 5 °C/min. Lettered arrows indicate temperatures at which X-ray diffraction experiments were performed (see Figure 9).

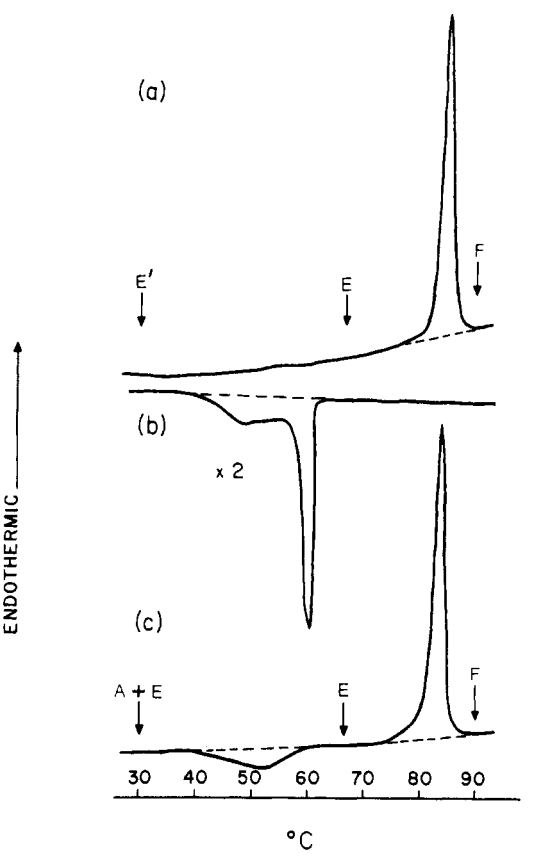

FIGURE 4: Differential scanning calorimetry of NPGS plus excess (70 wt %) water after prolonged storage, 1200 h, at 22 °C. (a) Initial heating scan, 5 °C/min; (b) cooling scan, 5 °C/min (×2 sensitivity); (c) subsequent heating scan immediately following cooling, 5 °C/min. Lettered arrows indicate temperatures at which X-ray diffraction experiments were performed (see Figure 9).

appear consistently when the NPGS–water system is heated and cooled at this rate. The first transition is exothermic and occurs over a broad temperature range (55–65 °C). The second event is a large endotherm at 82 °C of enthalpy 17.5 ± 1.0 kcal/mol. When the sample is cooled, as with the anhydrous lipid, there is a large hysteresis effect. The cooling scan in Figure 3b gives a complex exotherm. A sharp component, suggestive of a high cooperativity, occurs at 62 °C, while a broader transition occurs immediately after the sharp transition. The temperature range over which the broad transition occurs is 55–40 °C. The total enthalpy under both peaks is 8.5 ± 0.5 kcal/mol. The reheating scan, performed immediately after completion of the cooling scan, is shown in Figure 3c. The exothermic transition occurs over the temperature range 40–60 °C. The minimum excess specific heat occurs at slightly lower temperatures (52 °C) than in the initial heating scan (60 °C). Studies at different heating rates show that the peak temperature, extrapolated to an infinitely slow heating rate, is 52 °C. The large endothermic transition reoccurs at 82 °C, with a transition enthalpy identical with that observed in the initial heating run (Figure 3a).

The calorimetric behavior obtained for an NPGS–water sample which was equilibrated at room temperature for a prolonged period (1200 h) prior to heating is shown in Figure 4. The first heating scan (Figure 4a) shows no exothermic behavior between 40 and 60 °C. The high temperature endotherm occurs at 82 °C with an enthalpy of 17.5 ± 1.0 kcal/mol, identical with that for the sample described in Figure 3. Subsequent cooling gives the characteristic double exotherm (Figure 4b). Immediate reheating demonstrates behavior similar to the sample shown in Figure 3; that is, an exothermic transition occurs at ~52 °C. The enthalpy of this exotherm on heating the NPGS–water samples (see, for example, Figures 3a,c, 4a,c, and 5a,c) ranges from 0 to 8 kcal/mol, depending on both the rate of cooling and the time the sample is maintained at a low temperature before it is reheated over the 30–70 °C temperature range.

Figure 5 shows the effect of different heating and cooling rates. Figure 5a is the heating scan at 5 °C/min of a sample that had already been equilibrated above 82 °C. It is similar to the heating scans shown in Figures 3c and 4c. The cooling scan, however, was performed at a rate of 0.31 °C/min (Figure 5b). The enthalpy of the complex exothermic transition, which occurred in the 50–68 °C temperature range, is 17.5 ± 1.0 kcal/mol, equal to the enthalpy of the large transition at 82 °C on heating (Figure 5a). This is to be contrasted with the enthalpy of 8.5 ± 0.5 kcal/mol observed for the complex exotherm on cooling at 5 °C/min. Subsequent heating of the slowly cooled sample demonstrates no exothermic behavior in the 30–70 °C range, and only the large enthalpy transition at 82 °C is observed.

More detailed analysis of the calorimetric behavior over the 20–70 °C range of cerebroside in excess water with no preequilibration is given in Figure 6. The broad exothermic transition on heating at 5 °C/min is shown in Figure 6a. When the sample is cooled from 70 °C (Figure 6b) without passing through the endotherm at 82 °C, no calorimetric transition is detected. The subsequent heating scan (Figure 6c) demonstrates no transition, thus confirming the irreversibility of the exothermic event.

Samples of NPGS and water either equilibrated above 82 °C and cooled at rates ≤1.25 °C/min or stored at room

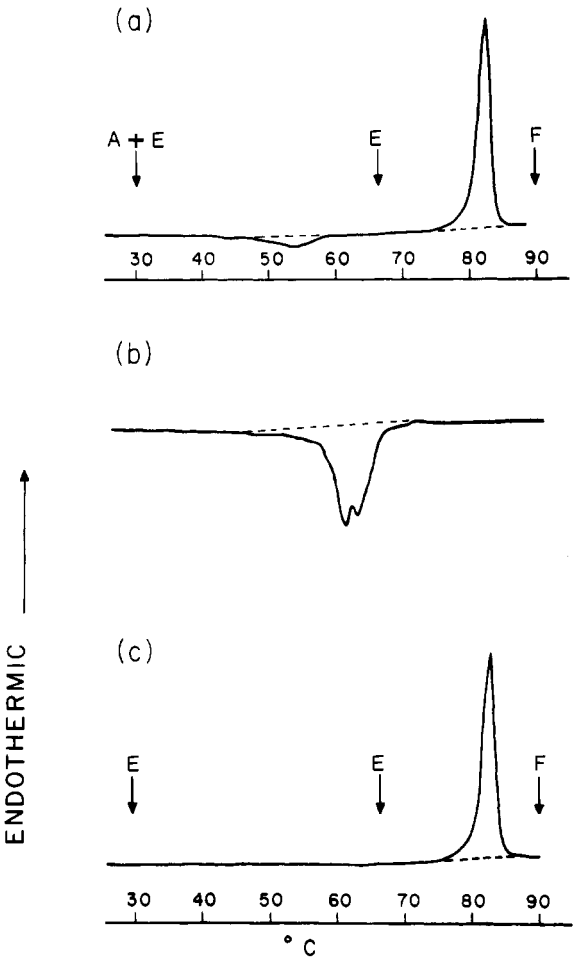

FIGURE 5: Differential scanning calorimetry of NPGS plus excess (70 wt %) water after equilibration at 90 °C and being cooled at 5 °C/min to 22 °C. (a) Initial heating scan, 5 °C/min; (b) cooling scan, 0.31 °C/min; (c) subsequent heating scan immediately following cooling, 5 °C/min. Lettered arrows indicate temperatures at which X-ray diffraction experiments were performed (see Figure 9).

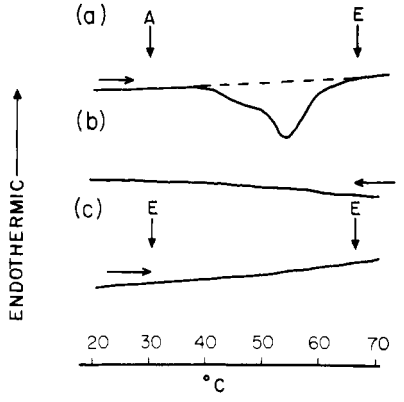

FIGURE 6: Differential scanning calorimetry of NPGS plus excess (70 wt %) water over the temperature range 20–70 °C. (a) Initial heating scan, 5 °C/min; (b) cooling scan, 5 °C/min; (c) subsequent heating scan immediately following cooling, 5 °C/min. Lettered arrows indicate temperatures at which X-ray diffraction experiments were performed (see Figures 9 and 10d).

temperature for prolonged periods (>600 h) also showed no detectable exothermic transition over the 20–70 °C temperature range. Thus, the appearance of this exotherm on heating immediately after the sample is rapidly cooled (5 °C/min) from a temperature above 82 °C suggests interconversions between stable and metastable forms.

The enthalpy of the exothermic transition is clearly dependent on the cooling rate (compare Figures 3b, 4b, and 5b).

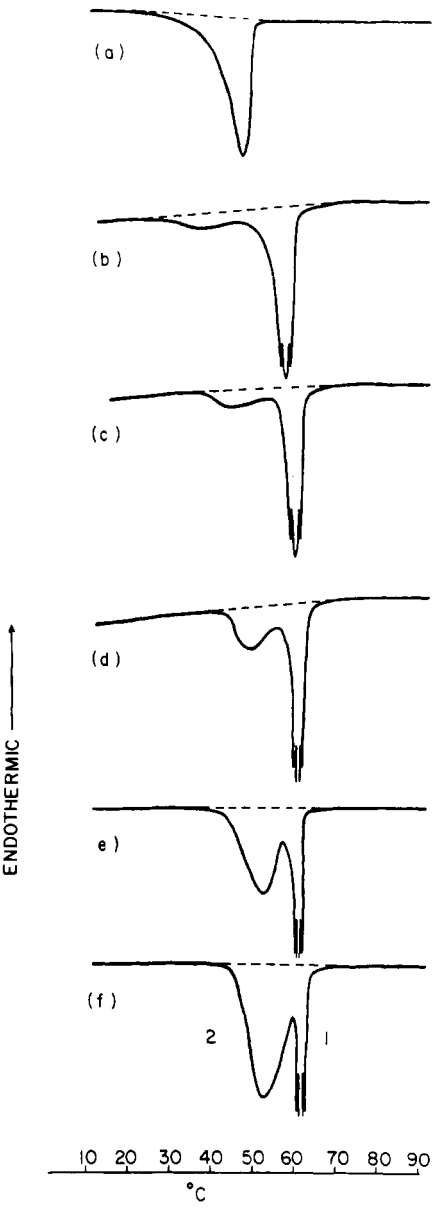

FIGURE 7: Differential scanning calorimetry of fully hydrated NPGS (70 wt % water). Effect of cooling rate on transition exotherms. Cooling rate: (a) 40, (b) 20, (c) 10, (d) 5, (e) 2.5, and (f) 1.25 °C/min.

Therefore, various cooling rates were used to quantitate the enthalpy of the complex, two-component exotherm observed on cooling. The fast cooling rates result in smaller enthalpies for the exothermic component (labeled 2) in the 30–58 °C range (Figure 7). For the sharper exotherm at ~61–63 °C (labeled 1), the enthalpy remains constant at 5.4 ± 0.5 kcal/mol at all cooling rates. The two-component cooling pattern is observed at all rates except at rates ≥40 °C/min, where only the single sharp exotherm 1 occurs, and at very slow rates ≤0.62 °C/min, where more complex exothermic peaks can be observed. The same two components, exotherms 1 and 2, however, are resolvable at these slow rates. The dependence of the transition enthalpies corresponding to exotherms 1 and 2 on cooling rate (Figure 8) shows clearly the constant contribution of exotherm 1 and the cooling rate dependent contribution of exotherm 2 to the total enthalpy change.

X-ray Diffraction. The lettered arrows in Figures 3–6 correspond to the X-ray diffraction patterns in Figure 9. When cerebroside and water are mixed at room temperature, the X-ray diffraction pattern recorded immediately is shown

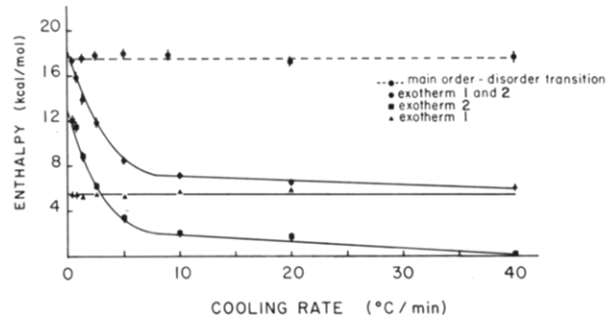

FIGURE 8: Dependence of transition enthalpies on cooling rate. (▲) Exotherm 1; (■) exotherm 2; (●) exotherm 1 + 2. Following cooling at these rates, the transition enthalpy observed at 82 °C is indicated (--●--).

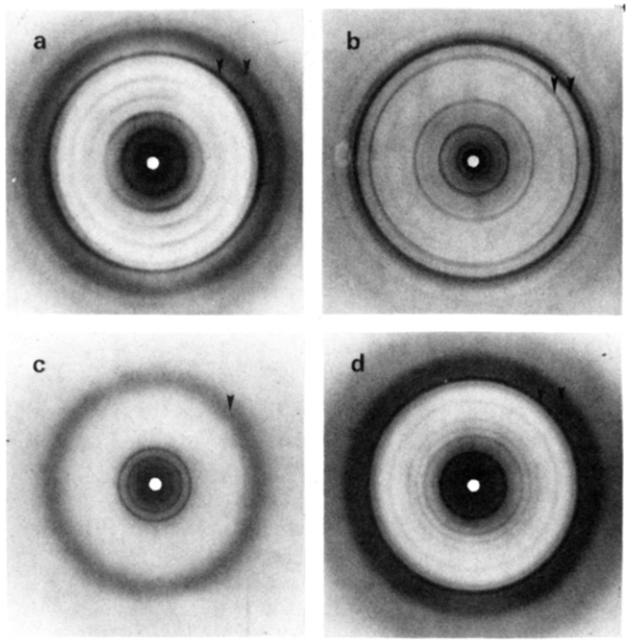

FIGURE 9: X-ray diffraction patterns of NPGS/water (70 wt %). (a) T = 30 °C, initial exposure within 72 h of sample preparation (anhydrous crystal A form in water); sample had not exceeded 30 °C; (b) T = 66 °C (hydrated crystal E form); (c) T = 90 °C, liquid crystal form F; (d) T = 30 °C (dehydrated crystal A and hydrated crystal E forms in water), after the sample was cooled (~5 °C/min) from 90 °C.

in Figure 9a. This diffraction pattern is identical with the anhydrous NPGS X-ray diffraction pattern (Figure 2a). The lamellar spacing is 58 ± 0.5 Å. This pattern is always obtained within 24–72 h after the sample is prepared at room temperature. Once the sample is heated past the exotherm to 66 °C (arrow E in Figure 3a), the diffraction pattern shown in Figure 9b is obtained. The 10 orders of small-angle reflections index according to a lamellar lattice of periodicity d = 54.5 ± 0.5 Å. A large number of reflections are observed in the wide angle region, the reflections at 1/4.6 and 1/4.1 Å^{-1} being the strongest. Continued heating beyond the main transition to 90 °C (arrow F in Figure 3a) results in a diffraction pattern characteristic of a liquid-crystalline state (Figure 9c). At this temperature, the wide angle region gives a broad, diffuse reflection centered at 1/4.6 Å^{-1}. This is characteristic of the disordered hydrocarbon chain packing in the "melted" state. Four small-angle reflections index on a lamellar lattice of periodicity d = 51.0 ± 0.5 Å.

After the sample is cooled at approximately 5 °C/min from 90 to 30 °C, the X-ray diffraction pattern at 30 °C shown in Figure 9d is observed. The small-angle reflections index on both the d ~58-Å lattice observed at 30 °C prior to heating

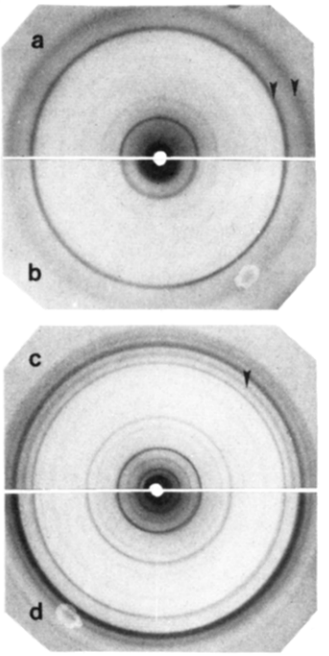

FIGURE 10: X-ray diffraction pattern of NPGS/water (70 wt %). (a) T = 30 °C, after the sample was rapidly cooled (~180 °C/min) to 30 °C; (b) T = 30 °C, anhydrous crystal A form; (c) T = 30 °C, sample as in (a) following prolonged incubation (480 h) at 30 °C; (d) T = 30 °C; sample had been heated to 66 °C and cooled to 30 °C (hydrated crystal E).

(Figure 9a) and the 54.5-Å lattice observed at 66 °C (Figure 9b). The wide angle region is characterized by a strong reflection at 1/4.55 Å^{-1} and a more diffuse reflection centered at 1/4.16 Å^{-1}.

X-ray diffraction experiments designed to explain the calorimetric data shown in Figure 6 (arrows A and E) demonstrate that once the diffraction pattern shown in Figure 9b is obtained by passing through the exotherm, this form is retained in subsequent cooling to 30 °C and reheating to 66 °C; i.e., this stable form persists at all temperatures below the major transition (<82 °C).

In a separate experiment, NPGS in the crystal form B′ was mixed with water at room temperature, and an X-ray diffraction pattern identical with the anhydrous crystal form B′ sample was obtained (Figure 2d). The initial heating of this sample to 70 °C in a calorimetric experiment gave an exothermic transition at 52 °C similar to that shown in Figure 3a. X-ray diffraction of this sample at 66 °C gave an identical pattern with the crystal form A–water sample when it is heated to 66 °C, i.e., the stable E form. These observations suggest a similarity in the molecular events as crystal form A and crystal form B′ transform to the stable E form structure in the presence of water.

The X-ray diffraction pattern of a hydrated NPGS sample rapidly cooled (~180 °C/min) from 90 to 30 °C was recorded at 30 °C (Figure 10a). This pattern is identical with that of the nonequilibrated NPGS–water system (Figure 9a) and also anhydrous NPGS (Figure 10b). The two predominant wide angle reflections are a strong reflection centered at 1/4.4 Å^{-1} and a broad reflection centered at 1/3.8 Å^{-1}. After the rapidly cooled sample is stored at room temperature for 480 h, the X-ray diffraction pattern shown in Figure 10c is obtained. There are close similarities between this pattern and the diffraction pattern from a sample cooled slowly from 66 °C to room temperature (see Figure 10d) or from samples examined once the exotherm is exceeded on heating (compare Figure 9b). The lamellar periodicities in Figure 10c,d are

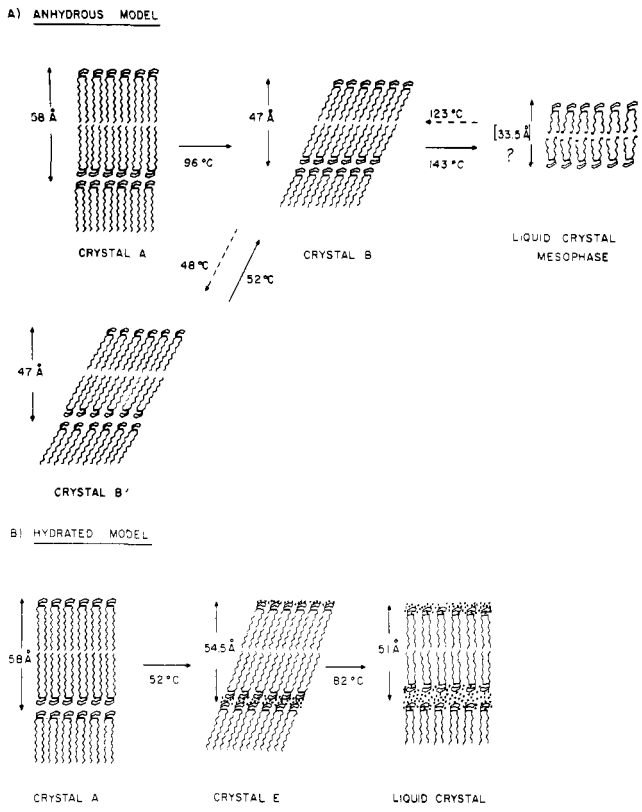

FIGURE 11: Schematic representation of the temperature-dependent structural changes in NPGS. (A) Anhydrous NPGS; (B) hydrated NPGS.

identical, 54.5 Å. The two strong wide angle reflections in Figure 10c,d at 1/4.6 and 1/4.1 $Å^{-1}$ are characteristically found in the stable E form (Figure 9b). The wide angle reflection at 1/4.4 $Å^{-1}$ corresponds to residual metastable form A (see arrow, Figure 10c).

Discussion

Anhydrous NPGS. In this study, anhydrous NPGS has been shown by X-ray diffraction, differential scanning calorimetry, and polarizing microscopy to exhibit complex polymorphic and mesomorphic behavior. The main features are summarized in Figure 11A.

The crystalline form initially observed at 23 °C, crystal form A, has a lamellar repeat, d = 58.0 Å (Figure 2a). The X-ray reflections are quite broad, indicating some disorder in the crystal, perhaps due to the mode of crystallization, solvent trapping, etc. When crystal form A is heated, an irreversible transition is observed at 96 °C (Figure 1a), and the overall diffraction pattern changes to that of a second "crystalline" form, crystal form B (Figure 2b). The number of reflections observed in the small angle region is reduced, and the lamellar periodicity decreases to 47.0 Å. The wide angle reflections consist of a sharp line centered at 1/4.4 $Å^{-1}$ which is overlapped by a more diffuse reflection. Although there are no gross morphological, textural, or viscosity changes observed under the polarizing microscope, the reduced number of lamellar reflections and the diffuse nature of the wide angle reflections suggest an even less ordered hydrocarbon chain packing lattice. Increased thermal energy at this high temperature (110 °C) would facilitate increased chain rotational motion and result in an increased average chain packing area. The increased chain disorder may, in part, explain the decreased lamellar spacing. However, a more likely explanation would be an alteration of the cerebroside molecular axis tilt relative to the bilayer normal (see Figure 11A). Similar irreversible transitions during the initial heating have been reported for other cerebrosides and glycosphingolipids (Abrahamsson et al., 1972). These various thermally induced crystal forms can also be obtained by crystallization from different solvents (Abrahamsson et al., 1972).

Heating the crystal form B beyond the 143 °C transition gives a diffraction pattern consisting of a single low-angle reflection at 1/33.5 $Å^{-1}$ (Figure 2c). This reflection and the middle texture observed by polarizing microscopy are consistent with a liquid-crystalline phase. The diffuse reflection at 1/4.6 $Å^{-1}$ is indicative of "melted" hydrocarbon chains. The observed spacing at 33.5 Å is similar to the value of 34 Å observed by Abrahamsson et al. (1972) for the liquid-crystalline C_{18}-cerebroside. However, the observation of only a single reflection does not allow the liquid-crystal lattice type (lamellar, hexagonal, etc.) to be defined. The arrangement depicted in Figure 11A is meant only to represent this class of thermotropic liquid-crystal structures.

The transition at 180 °C is shown by polarizing microscopy to be the liquid-crystal → isotropic liquid melt. The transition is reversible. Various geometrical forms typical of a middle liquid-crystalline mesophase are observed on cooling (e.g., fanlike texture, striated texture). Although the liquid-crystal → crystal B transition is reversible on cooling, it exhibits marked hysteresis, occurring approximately 20 °C below the transition temperature observed on heating. No further transitions occur on cooling until 48 °C, where the crystal form B transforms to a new crystal form B′ (Figure 2d). This crystal form has the same lamellar spacing of 47.0 Å and intensity distribution of the low angle reflections as crystal form B, but differences are observed in the wide angle region. The increased number of sharp reflections indicates a more ordered crystal form. Formation of a more ordered structure with a specific hydrocarbon chain packing arrangement would be consistent with the exothermic transition observed on cooling at 48 °C by DSC (Figure 1b). X-ray reflections at 1/4.5, 1/3.85, and 1/4.2 $Å^{-1}$ suggest a chain packing similar to the hybrid type subcells reported for dilauroyl-DL-phosphatidylethanolamine (Hitchcock et al., 1974; Elder et al., 1977) and β-D-galactosyl-*N*-(2-D-hydroxyoctadecanoyl)-D-*erythro*-dihydrosphingosine (Pascher & Sundell, 1977).

The irreversible transition at 96 °C, the transition at 143 °C (Figure 1a), and the transition at 48 °C (Figure 1c) correspond to similar polymorphic conversions observed by X-ray diffraction for synthetic C_{18}-cerebroside (Abrahamsson et al., 1972). A similar pattern of changes in the lamellar periodicities occurs for the two related compounds. Furthermore, temperature-dependent polymorphic behavior has been observed by X-ray diffraction for the naturally occurring bovine brain cerebroside hydroxy fatty acid containing (phrenosine) and nonhydroxy fatty acid containing (kerasine) subfractions (Fernandez-Bermudez et al., 1977; Hosemann et al., 1979).

Hydrated NPGS. The thermotropic behavior of NPGS differs markedly from that of synthetic membrane phospholipids such as phosphatidylcholine. A summary of the structural changes is shown in Figure 11B while a scheme emphasizing the thermodynamic changes and the stability/metastability of the different forms is shown in Figure 12.

The calorimetric scans in Figures 3 and 6 demonstrate that in the presence of excess water the initial heating over the 20–70 °C range results in an exothermic transition at 52 °C. Cooling from 70 °C to room temperature shows no crystal form E → crystal form A thermal transition, and no transition is obtained when the sample is reheated over the same tem-

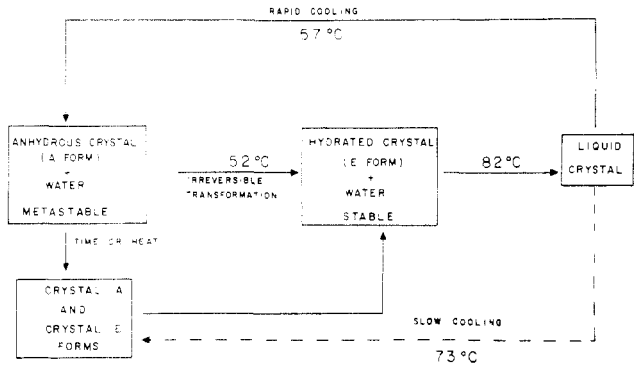

FIGURE 12: Interconversions of stable, metastable, and liquid-crystalline states of hydrated NPGS.

perature range (Figure 6). The excess negative enthalpy of the initial exotherm suggests the transition from a metastable A form to a more stable state. The X-ray diffraction pattern typical of this stable E form (Figure 9b) at temperatures exceeding the exotherm is also observed on cooling to 30 °C and on reheating to any temperature below 82 °C. Thus, the identical diffraction pattern observed at all temperatures below 82 °C is consistent with the exotherm involving an irreversible transformation to a more stable structure. The lamellar spacing of the stable hydrated NPGS form is reduced from 58.0 Å in crystal form A to 54.5 Å in the stable E form, suggesting a change in the molecular tilt with respect to the bilayer normal as indicated in Figure 11B. The presence of a number of sharp reflections in the wide angle region indicates a more ordered hydrocarbon chain packing arrangement than that exhibited by the hydrated gel forms of phospholipids such as lecithin (Janiak et al., 1979). X-ray diffraction evidence for a similarly ordered hydrocarbon chain packing mode has been demonstrated recently for *N*-stearoylsphingomyelin (Estep et al., 1980). The stable E structure does not correspond to any of the polymorphic forms observed in the anhydrous system. Clearly, it requires the presence of water for its formation, suggesting a molecular interaction between water and the galactosyl residue.

Following prolonged incubations of water and NPGS at room temperature, no exothermic behavior is detected over the temperature range preceding the 82 °C transition. Also, the X-ray diffraction pattern at room temperature shows initially a number of small-angle reflections indexing on lamellar lattices corresponding to both the nonhydrated crystal form A–water sample (58 Å) and the stable hydrated form E (54.5 Å) (Figures 2a and 9b). Similarly the changes occurring in the wide angle region, particularly the appearance of a strong reflection centered at $1/4.04$ Å^{-1}, are indicative of conversion to a similar hydrocarbon chain arrangement to that present in the stable E form. With increasing incubation time, the observed diffraction pattern becomes progressively dominated by that corresponding to the stable E form. It is therefore concluded that conversion to the stable state involves a time-dependent hydration process involving interaction of water with the polar head group and a concomitant reordering of the hydrocarbon chain packing. The solution of simple monosaccharides in water yields a negative free-energy change, indicating that there is a strong hydrogen bonding between the sugar hydroxyl groups and water molecules. This binding is apparently stronger or more abundant than that between water molecules themselves (Taylor & Rowlinson, 1955). Similar thermodynamic considerations may apply to the interaction of the sugar moiety of the NPGS head group with water as the latter absorbs onto and eventually penetrates into the polar matrix. A similar exothermic transition on heating has been observed for natural glucocerebroside from Gaucher's spleen and synthetic *N*-palmitoylglucocerebroside (Freire et al., 1980). These workers conclude that the exothermic transition corresponds to a conversion to a more stable crystal state involving a rearrangement of the hydrocarbon chain packing. We further suggest that this chain packing alteration is accompanied by rehydration of the lipid.

The exothermic behavior observed during heating scans does not reoccur until the liquid-crystal phase transition is exceeded and the sample rapidly cooled. This suggests a time-dependent molecular rearrangement that can be elucidated by looking at both the liquid-crystal Lα state and the rate of cooling from this "melted" state. The X-ray diffraction (Figure 9c) and calorimetric (Figure 3c) data indicate that the main thermal transition at 82 °C is associated with the energy required to melt the hydrocarbon chain moieties with the formation of the liquid-crystalline Lα structure. However, this chain melting process for NPGS involves an unusually high enthalpy change (ΔH = 17.5 kcal/mol). High enthalpy transitions have also been observed for other cerebroside (Freire et al., 1980; Bunow, 1979; Bunow & Levin, 1980) and sphingomyelin (Estep et al., 1980) dispersions. In contrast, the C_{16}-phospholipid (dipalmitoylphosphatidylcholine) undergoes a hydrocarbon chain order–disorder (gel–liquid crystalline) transition at 41.6 °C with an enthalpy of 8.7 kcal/mol (Chapman et al., 1967; Janiak et al., 1976, 1979). Thus, the transition enthalpy of the cerebroside is approximately twice that of an equivalent chain length of phospholipid, indicating that additional energy constraints must be overcome on passing from the stable E form to the liquid-crystalline (Lα) state. Further insight into the high temperature, high enthalpy transition of NPGS may be obtained through a closer examination of the complexity of the hydrocarbon moieties, the nature of the polar group, and its intra- and intermolecular interactions, utilizing information from the crystal structure of cerebroside (Pascher & Sundell, 1977).

The cerebroside molecule contains the N-acylated fatty acid and sphingosine chain that extend into the hydrophobic bilayer region. The sphingosine moiety contains two molecular groups which are present at the interface region between the lipid hydrocarbon domain and the polar (galactosyl) head group. First, the amide group has a planar conformation and the potential to be involved in intra- or intermolecular hydrogen bonding as both donor and acceptor. Second, the hydroxyl group at C_3 has been shown to form intermolecular hydrogen bonds with adjacent cerebroside molecules (Pascher & Sundell, 1977). Furthermore, the galactosyl group has an extensive hydrogen-bonding network extending laterally over the bilayer interface. It has been suggested that hydrogen bonds involving both the hydrophilic sugar matrix and the amide and hydroxyl groups of the sphingosine base can contribute 3–10 kcal/mol of bond energy to the lateral lipid–lipid interaction and thus considerably increase the stability of the bilayer (Pascher, 1976). Support for the involvement of hydrogen bonding in the galactose region of hydrated NPGS comes from the study of Skarjune & Oldfield (1979). ^{2}H NMR studies of hydrated NPGS with the deuterium labeled C_6-galactose reveal a slow hydroxymethyl group motion on the ^{2}H NMR time scale ($>10^{-5}$ s) at all temperatures below 82 °C, consistent with involvement of this group in a hydrogen bonding network. Hydrogen bonding in the hydrated crystal state has been demonstrated by a recent Raman study of bovine brain cerebroside kerasine and phrenosine subfractions (Bunow & Levin, 1980). Additional intermolecular interactions of this

type may facilitate the formation of more ordered chain packing modes and increase the overall stability of the NPGS structure. This, in turn, will influence the thermodynamic characteristics of the chain melting transition.

As observed by X-ray diffraction and polarizing light microscopy above 82 °C, a hydrated lamellar liquid crystal is formed from the stable E form. At this transition, lateral expansion of the lipid bilayer and an increased surface area per NPGS molecule at the lipid–water interface result from an increasing disorder of the hydrocarbon chains. The decrease in the lamellar dimension from 54.5 to 51 Å is consistent with lateral bilayer expansion. This lateral expansion and increased surface area per molecule presumably allows more water to enter into the interbilayer region. Disruption of hydrogen bonding between adjacent NPGS molecules will occur as the entering water molecules compete at intermolecular lipid–lipid hydrogen bond sites.

As the hydrated NPGS liquid crystal is cooled, a supercooling effect of 9–16 °C occurs which is dependent on the rate of cooling. The supercooling phenomenon may result from the persistence of intercalated water molecules in the head group–interface region. These water molecules continue to participate in a hydrogen bonding matrix, thus maintaining an increased head-group surface area. This would allow the hydrocarbon chains to remain in a disordered state even when the temperature of the system is below 82 °C. At very slow cooling rates, the maximum temperature at which the dehydrated crystalline form A appears is 73 °C. Maintaining the supercooled NPGS liquid crystal in an isothermal mode at or above 73 °C for extended periods (24–36 h) results in no liquid-crystalline → crystal transition. At cooling rates between 20 and 1.25 °C/min, the liquid-crystalline → crystal transition shows a two-component exothermic transition (exotherms 1 and 2 in Figure 7). Decreasing cooling rates give an increased enthalpy for exotherm 2, and a linear extrapolation to zero cooling rate gives an intercept of 12.8 kcal/mol (Figure 8). The increase of total enthalpy for the entire transition paralleled the behavior of exotherm 2 until at very slow heating rates the total transition enthalpy was the same as the enthalpy of the chain transition on heating, 17.5 kcal/mol (crystal form E → liquid crystal).

The X-ray diffraction pattern at 30 °C obtained after the sample is cooled from the liquid-crystalline state at 5 °C/min (Figure 9d) shows diffraction lines in the low angle and wide angle regions characteristic of both the nonhydrated NPGS–water (crystal form A) and the stable form E structures. This indicates that cooling through the complex exothermic transition results in the formation of both structures. This heterogeneity is substantiated by the X-ray diffraction patterns obtained following cooling at different rates from temperatures above 82 °C. After the sample is cooled at decreasing rates, the relative intensities of the reflections characteristic of the stable form E structure (Figure 10d) increase. Conversely, the reflections characteristic of the dehydrated crystal form A increase after rapid cooling rates. Following cooling at a rate greater than the extrapolated rate limit at which exotherm 2 can occur (Figure 8), a diffraction pattern identical with that of crystal form A results (Figure 10a,b). One of the effects occurring at the exothermic cooling transition is the loss of water from the NPGS bilayer. Furthermore, this effect appears to be associated with exotherm 1. After 20 days at room temperature (22–25 °C), the X-ray diffraction pattern characteristic of the stable E form is reestablished. This behavior is identical with that of the NPGS–water mixtures equilibrated for increasing times at room temperature.

A thermodynamic model summarizing the behavior of the NPGS/water system is shown in Figure 12. Crystal form E is the most stable form present at all temperatures below 82 °C. Heating beyond the transition at 82 °C yields the liquid-crystalline state (Lα). The behavior observed on cooling from the liquid-crystalline state depends critically on the cooling rate. If hydrated NPGS is cooled very rapidly, only the dehydrated metastable form A–water system results. At intermediate cooling rates, both the metastable form A and the stable form E are observed. The metastable A form transforms to the stable E form only by heating through the exotherm at higher temperatures or by prolonged incubation at room temperature. At very slow cooling rates, the conversion of the metastable form A to the stable form E occurs within the time scale of the experiment, and only the stable form E is observed at low temperatures.

Summary

The following general hypothesis is suggested (see Figures 11B and 12). Cerebroside (NPGS) when mixed with water hydrates slowly at room temperature. This slow hydration may be due to a tightly packed interfacial region with an effective galactose–galactose head group hydrogen-bonding matrix. Water penetration of this matrix is accelerated by heating, with the exotherm at 52 °C marking both the hydration process and the conversion to the stable form E. Hydrogen-bond formation between water molecules and galactose head groups would result in a stabilizing hydrogen-bonding matrix at the lipid–water interface region. The transition from the stable E form to the liquid-crystalline state Lα disrupts both the very stable hydrocarbon chain packing and the intermolecular hydrogen-bond interaction. The transformation back to the stable E form may not occur until the liquid crystal recondenses its hydrocarbon chains, eliminates excess water, and forms the dehydrated crystal A form. This form must have the appropriate geometry for the reestablishment of the hydrogen-bond matrix of the stable form. At fast cooling rates, the chain packing mode characteristic of the crystal form A is produced, and water of hydration appears to be excluded from the structure. Thus, the head group–head group, inter- and intramolecular associations stabilizing the dehydrated metastable form A result. Rehydration and conversion to the stable E form is a time-dependent, temperature-dependent phenomenon. The formation of the stable E form on slow cooling represents a liquid crystal → metastable form A → stable form E process. Slow cooling of Lα to crystal form A allows sufficient time at high temperatures for form A to completely convert to the stable hydrated form. This complex behavior observed for NPGS underlines the importance of a combined structural and thermodynamic approach to the study of these complex polar lipids where irreversible transitions, formation of metastable states, etc., are now being observed [see also Estep et al. (1980) and Freire et al. (1980)].

Acknowledgments

We acknowledge the assistance of Irene Miller in the preparation of this manuscript.

References

Abrahamsson, S., Pascher, I., Larsson, K., & Karlsson, K. A. (1972) *Chem. Phys. Lipids 8*, 152–179.

Abrahamsson, S., Dahlén, B., & Pascher, I. (1977) *Acta Crystallogr., Sect. B B33*, 2008–2013.

Barenholz, Y., Suurkuusk, J., Mountcastle, D. B., Thompson, T. E., & Biltonen, R. L. (1976) *Biochemistry 15*, 2441–2447.

Brady, R. O. (1978) in *The Metabolic Basis of Inherited Disease* (Stanbury, J. B., Wyngaarden, J. B., & Fredrickson, D. E., Eds.) pp 718-746, McGraw-Hill, New York.
Bunow, M. R. (1979) *Biochim. Biophys. Acta 574*, 542-546.
Bunow, M. R., & Levin, I. W. (1980) *Biophys. J. 32*, 1007-1021.
Calhoun, W. I., & Shipley, G. G. (1979) *Biochemistry 18*, 1717-1722.
Chapman, D., Williams, R. M., & Ladbrooke, B. D. (1967) *Chem. Phys. Lipids 1*, 445-475.
Clowes, A. W., Cherry, R. J., & Chapman, D. (1971) *Biochim. Biophys. Acta 249*, 301-317.
Correa-Freire, M. C., Freire, E., Barenholz, Y., Biltonen, R. L. & Thompson, T. E. (1979) *Biochemistry 18*, 442-445.
Curatolo, W., Small, D. M., & Shipley, G. G. (1977) *Biochim. Biophys. Acta 468*, 11-20.
Dahlén, B., & Pascher, I. (1972) *Acta Crystallogr., Sect. B B28*, 2396-2404.
Elder, M., Hitchcock, P., Mason, R., & Shipley, G. G. (1977) *Proc. R. Soc. London, Ser. A A354*, 157-170.
Elliot, A. J. (1965) *J. Sci. Instrum. 42*, 312-316.
Estep, T. N., Calhoun, W. I., Barenholz, Y., Biltonen, R. L., Shipley, G. G., & Thompson, T. E. (1980) *Biochemistry 19*, 20-24.
Fernandez-Bermudez, S., Loboda-Cackovic, J., Cackovic, H., & Hosemann, R. (1977) *Z. Naturforsch. C: Biosci. 32C*, 362-374.
Fishman, P. H., & Brady, R. O. (1976) *Science (Washington, D.C.) 194*, 906-915.
Freire, E., Bach, D., Correa-Freire, M., Miller, I., & Barenholz, Y. (1980) *Biochemistry 19*, 3662-3655.
Hitchcock, P. B., Mason, R., Thomas, K. M., & Shipley, G. G. (1974) *Proc. Natl. Acad. Sci. U.S.A. 71*, 3036-3040.
Hosemann, R., Loboda-Cackovic, J., Cackovic, H., Fernandez-Bermudez, S., & Balta-Calleja, F. J. (1979) *Z. Naturforsch. C: Biosci. 34C*, 1121-1124.
Huang, T. H., Skarjune, R. P., Wittebort, R. J., Griffin, R. G., & Oldfield, E. (1980) *J. Am. Chem. Soc. 102*, 7377-7379.
Janiak, M. J., Small, D. M., & Shipley, G. G. (1976) *Biochemistry 15*, 4575-4580.
Janiak, M. J., Small, D. M., & Shipley, G. G. (1979) *J. Biol. Chem. 254*, 6068-6078.
Johnson, A. C., McNabb, A. R., & Rossiter, R. J. (1948) *Biochem. J. 43*, 578-580.
Lapetina, E. G., Soto, E. F., & DeRobertis, E. (1968) *J. Neurochem. 15*, 437-445.
McCabe, P. J., & Green, C. (1977) *Chem. Phys. Lipids 20*, 319-330.
Neuringer, L. J., Sears, B., & Jungalwala, F. B. (1979) *FEBS Lett. 104*, 173-175.
Oldfield, E., & Chapman, D. (1972) *FEBS Lett. 21*, 303-306.
Pascher, I. (1976) *Biochim. Biophys. Acta 455*, 433-451.
Pascher, I., & Sundell, S. (1977) *Chem. Phys. Lipids 20*, 175-191.
Reiss-Husson, F. (1967) *J. Mol. Biol. 25*, 363-382.
Rosevear, F. (1954) *J. Am. Oil Chem. Soc. 31*, 628-639.
Shipley, G. G., Avecilla, L. S., & Small, D. M. (1974) *J. Lipid Res. 15*, 124-131.
Skarjune, R., & Oldfield, E. (1979) *Biochim. Biophys. Acta 556*, 208-218.
Taylor, J. B., & Rowlinson, J. S. (1955) *Trans. Faraday Soc.*, 1183-1192.
Untracht, S. H., & Shipley, G. G. (1977) *J. Biol. Chem. 252*, 4449-4457.

Detailed Analysis of the Nucleosomal Organization of Transcribed DNA in Yeast Chromatin†

D. E. Lohr

ABSTRACT: The precise chromatin structure of actively transcribed DNA in yeast has been analyzed by electrophoretic transfer of high-resolution staphylococcal nuclease and DNase I chromatin digest DNA patterns to DBM paper and hybridization with active sequence probes. The DNA patterns of the transcribed DNA sequences resemble the DNA patterns produced by digestion of bulk yeast nucleosomes. Hence, these active sequences must be arranged in "typical" nucleosome structures. Furthermore, in details of the structure, the active sequence nucleosomes look almost exactly like the average yeast nucleosome in repeat length, in the length of DNA associated with the core particle, in the amount and type of heterogeneity found within and between the oligomeric and monomeric repeat lengths of DNA, in the occurrence of discrete spacer lengths including the characteristic five nucleotide increments (i.e., 5, 15, 25, ... base pairs), and in the length of DNA between yeast nucleosomes. Early in digestion, there are some differences: increases in peak breadths (i.e., in the distribution of spacer lengths) and some preferential release of monomer DNA. These results suggest that transcribed DNA can exist in the typical (yeast) type of nucleosome organization and thus that active chromatin regions do not necessarily require profound structural rearrangements. The slight differences noted are consistent with some slight, mainly spacer, modification in the vicinity of the transcription event itself.

The basis of the selectivity of eukaryotic transcription and its relationship to the presence and the properties of nucleosomes remains unknown despite intense study (Mathis et al., 1980). The current model, largely on the basis of work with chicken globin and ovalbumin (Mathis et al., 1980), envisions that active genes do in fact contain nucleosomes whose structure is subtly yet distinctly altered with respect to nonactive nucleosomes, an alteration which, for example, is reflected in an increased susceptibility to DNase I digestion (Weintraub & Groudine, 1976).

† From the Chemistry Department, Arizona State University, Tempe, Arizona 85287. *Received April 6, 1981.* This work was supported by National Institute of General Medical Sciences Grant 27623.

0006-2960/81/0420-5966$01.25/0